Water Resources Research

RESEARCH ARTICLE
10.1029/2018WR024025

Key Points:
- For a given total thickness of a two-layered soil the thickness of the upper layer minimizing or maximizing evaporation flux is found
- Gardner's, Philip's, and van Genuchten's soils are studied in 1-D flows from a static water table to dry topsoil
- Analytical solutions of Richards ODEs are juxtaposed with HYDRUS finite element computations

Correspondence to:
A. R. Kacimov,
anvar@squ.edu.om;
akacimov@gmail.com

Citation:
Kacimov, A. R., Obnosov, Y. V., & Šimůnek, J. (2019). Minimizing evaporation by optimal layering of topsoil: Revisiting Ovsinsky's smart mulching-tillage technology via Gardner-Warrick's unsaturated analytical model and HYDRUS. *Water Resources Research*, *55*. https://doi.org/10.1029/2018WR024025

Received 3 SEP 2018
Accepted 11 MAR 2019
Accepted article online 21 MAR 2019

©2019. American Geophysical Union.
All Rights Reserved.

Minimizing Evaporation by Optimal Layering of Topsoil: Revisiting Ovsinsky's Smart Mulching-Tillage Technology Via Gardner-Warrick's Unsaturated Analytical Model and HYDRUS

A. R. Kacimov[1], Yu.V. Obnosov[2], and J. Šimůnek[3]

[1]Department of Soils, Water and Agricultural Engineering, Sultan Qaboos University, Muscat, Oman, [2]Institute of Mathematics and Mechanics, Kazan Federal University, Kazan, Russia, [3]Department of Environmental Sciences, University of California, Riverside, CA, USA

Abstract Ovsinsky (1899, https://www.rulit.me/books/novaya-sistema-zemledeliya-read-193251-1.html) suggested and tested a water conserving soil no-till technology for rain-snow-fed field crops in a semiarid environment in southern Russia. We model Ovsynsky's unsaturated flow fragment, in which 1-D steady evaporation and evapotranspiration through a two-layered soil from a horizontal static water table to a dry soil surface takes place. Gardner's exponential and algebraic functions are used for the unsaturated hydraulic conductivity-suction head relations. The vertical evaporation flux depends on the dyads and triads (correspondingly) of the parameters of these functions, for example, the saturated hydraulic conductivity and the sorptive number of the two layers. The flux, as a function of the relative thickness of the upper stratum, is analytically found from the solution of one or two nonlinear equations. This relation can be nonmonotonic and exhibits either a minimum or maximum depending on whether this stratum is coarser or finer than the subjacent stratum fed from a horizontal isobar. HYDRUS-1D simulations confirm these extrema. This explains the experimental results from the literature on mulching/tillage/soil crusting-sealing, which can increase, decrease, or have no impact on evaporation from a shallow water table. Alterations of the soil's homogeneity to reduce evaporation losses can improve the hydrological balance of soil profiles.

1. Introduction

Crop fields are sometimes cultivated on soils with a shallow freshwater table (line W_1W_2 in Figure 1). This isobar is maintained either naturally by groundwater from an unconfined aquifer or by Kornev's (1935) subsurface irrigation. Hydrologically, such agro-engineering system illustrates the water use efficiency-constrained dichotomy: soil water should be available to plant roots for transpiration, while evaporation from the soil surface (line S_2S_1 in Figure 1), with ensued secondary salinization, is deleterious to the agro-environment. The dilemma, formulated as an optimal control problem, is how to maximize (or maintain at the level of physiological requirements of a particular crop) the former and minimize the latter. In 1899, the Russian agronomist and philosopher Ovsinsky (It is noteworthy that Ovsinsky had to change even the title of some chapters of his book because of the animosity from his opponents in the academia. For example, his original title for section 1 of the book can be translated as "Self-reflection of plants" or even "Ontological endeavours of plants." Ovsinsky considered plants as biological creatures having a higher level of organization than animals (including Aristotelian animals). Ovsinsky drew the following political analogy: plants are republics and animals are monarchies. In the book, Ovsinsky also suggested to upgrade even the terminology: *agronomy* -> *husbandry* of plants as conscious and even intelligent creatures. Ovsinsky perpended on plants as creatures cognizant of farmer's agronomic actions. These Ovsinsky's ideas were vehemently opposed by the contemporaneous crop/plant scientists.) suggested and tested the technology of a no-till treatment of topsoil in semiarid crop fields. The main idea was very simple: to convert an initially homogeneous (quasi-homogeneous) soil body of a given thickness D between W_1W_2 and S_2S_1 into a two-layered composite (Figure 1). The plant roots uptake moisture from this composite, which is agronomically favorable. Evaporation from the soil surface, although relatively less (as compared with surface irrigation), is bad because it reduces the water use efficiency and causes secondary salinization, among other negative

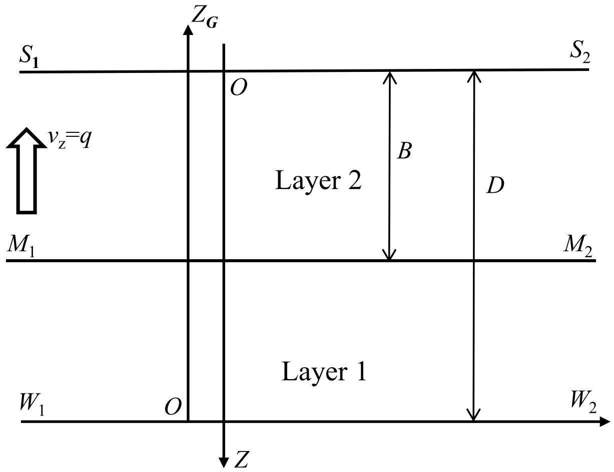

Figure 1. Two-layered soil with a vertical ascending evaporative flux from the water table at a depth D. Two vertical axes are as follows: Philip's OZ is oriented downward and OZ_G is oriented upward. B is the thickness of the upper layer.

consequences. The Ovsinsky's thickness D of the unsaturated zone in Figure 1 was high enough to serve as an antievaporation sheath. This partially saturated layer also served in Ovsinsky's agronomy as a thermal insulator for the plant roots, provided they penetrate deeply from the superheated soil surface. This dual *smart* wetting and heat-stress mitigation of the unsaturated layer has been corroborated by numerous data on improved harvest/biomass/plant morphologies for a variety of crops.

Mathematically, Ovsinsky (1899) minimized the evaporative flux, q, by making the hydrophysical parameters of a layer 2 of thickness B (Figure 1) different from those of the original soil (layer 1). From this viewpoint, historically, crop cultivation by practices including tillage, viz., plowing, harrowing (post-plowing dragging of a heavy frame set with teeth or tines to break up soil clods), spudding (rooting-digging out weeds by a sharp spadelike tool), mulching, and treatment of the topsoil with polymers, among others.

After most treatments, the topsoil of thickness B (Figure 1) becomes coarser than a substratum of thickness D-B (see, e.g., Bodner et al., 2015, Connolly, 1998, Fuchs & Hadas, 2011, Hillel et al., 1975, Mehari et al., 2011, Minhas et al., 1986, Strudley et al., 2008, Verburg et al., 2012). Rains or intensive sprinkling produce an opposite effect: a thin (few mm) soil crust (seal) forms due to the impact of water drops on a relatively fine bare soil surface (see, e.g., Mualem & Assouline, 1989). The natural morphing of soils also results in a similar vertical stratification caused by illuviation, eluviation, lessivage, and cyanomat-lichen-moss development, among others (see, e.g., Felde et al., 2014), which evolve over decades to centuries unlike a commonly annual soil treatment in agronomy. In any type of heterogenization, the engineered or natural porous rectangle $M_1M_2S_2S_1$ has hydraulic and capillary properties that sharply or continuously contrast with those of the original subjacent soil in the rectangle $W_1W_2M_2M_1$ (Figure 1).

In this paper, we consider ascending steady unsaturated flow (Figure 1) from an isobaric horizon W_1W_2 through a two-layered rectangle $W_1W_2S_2S_1$. We use the unsaturated conductivity functions of Gardner (1958), Willis (1960), Warrick (1988), and van Genuchten (1980) for analyzing the relation $q(B)$. We use modern computer algebra routines to integrate and solve systems of nonlinear equations and find extrema of $q(B)$. We also simulate evaporation for the system in Figure 1 using HYDRUS-1D (Šimůnek et al., 2016). We assume that flow is Darcian, one-phase (vapor/gas and solute motions, depositions, and dissolutions are neglected), and isothermal and that the stratified soils are isotropic (Warrick, 2003).

We answer the following two (main) questions:

1. For a given texture (hydraulic and capillary properties) of each of the two strata in Figure 1 and for a fixed D, is there an optimal depth B that minimizes the losses q?
2. For fixed B and D, can one optimize the texture of the upper layer with an objective of reducing q?

It is noteworthy that for saturated steady flows for which the governing equation is linear, similar optimization problems have been recently analytically solved for 2-D flow (Kacimov & Obnosov, 2018). For unsaturated flows studied below, the nonlinearity of the governing (Richards) equations makes 2-D analytical solutions in composite soils prohibitively complex.

2. Analytical Solutions

As in Gardner (1958), Warrick (1988), and Willis (1960) we assume that along W_2W_1 in the first soil layer, the pressure head $p_1 = 0$. Moisture is lifted by the capillarity of two layers from W_2W_1 to a dry soil surface. Gravity and the Darcian resistance of both layers oppose the evaporation-maintained suction.

For most rain-fed and traditionally irrigated soils in agronomy and land surfaces of arid catchments in hydrology, evaporation is a transient 2–3 stage process (actually, a phase in soil water redistribution). The boundary conditions for moisture content or suction pressure at S_1S_2 in real fields vary with time, depending on plants' physiological stages and root evolution, atmospheric conditions (relative humidity of the air, its temperature, wind speed, and solar radiation), desiccation of the topsoil and fluctuations in the locus of the water table (see e.g., Boast & Simmons, 2005; Jalota & Prihar, 1990; Stewart & Broadbridge, 1999). In models, this requires solving nonlinear transient partial differential equations (PDEs) for each soil layer, taking into account generally hysteretic constituting relations (phase relative permeabilities and capillary pressure functions) imbedded in those PDEs. Consequently, simplifications and approximations of the corresponding boundary value problems (hereafter abbreviated as BVPs) are common (e.g., see Assouline et al., 2014; De Luca & Cepeda, 2016; Warrick, 1988). Field and laboratory studies of transient evaporation are performed using lysimeters, tensiometers, theta-probes, sigma-probes, thermometers, and other instruments to measure and assess moisture, solute, and temperature dynamics in soils. Mathematical models combine soil physics, shallow aquifer hydrology, and the near-surface atmosphere (e.g., see Al-Shukaili, 2018; Ehlers & Van Der Ploeg, 1976; Geng & Boufadel, 2015; Hillel & Talpaz, 1977; Khan, 1988; Li et al., 2016; Malik et al., 1992; Novák, 2012; Sadeghi et al., 2014; Soylu et al., 2011; Xiao et al., 2010; Zarei et al., 2010). Civil engineers most often ignore the plants and address the transient desiccation of clay liners. Engineers solve the same BVPs as agronomists but are mainly interested in cracking of layer 2 (in Figure 1); for them, q is of a minor concern. Correspondingly, their models of unsaturated flows with evaporation utilize PDEs that account for soil swelling and shrinkage (see, e.g., Zhou & Rowe, 2005).

As in Gardner (1958), we assume that the soil surface S_1S_2 has a constant negative pressure head $p_2 = -p_s$ and that $p_s = \text{const} > 0$. Gardner (1958) suggested several simple equations $k(S)$ for the unsaturated hydraulic conductivity k as a function of the suction head, S (p = -S), which were followed by the Brooks-Corey, Campbell, Fredlund, Kosugi, van Genuchten-Mualem, and other empirical $k(S)$ functions. Below, we answer a question from the Introduction by selecting two Gardner's formulas, viz., exponential and algebraic $k(S)$ functions, which we call the G-E and G-A equations (in Gardner, 1958, equations (8) and (11), correspondingly).

Gardner and Fireman (1958) stated that "… the steady-state rate of evaporation from a soil surface mulch should be inversely proportional to the thickness of the mulch" and experimentally quantified this monotonic reduction in evaporation (see Figure 7 in their paper). However, in their experiments, D was not fixed, and the observed decrease in q due to adding more sand on the top of loam seems trivial. Similarly, a decrease in evaporation through homogeneous or layered soils when the water table in Figure 1 drops, i.e., D increases (see also Ripple et al., 1970, their Figure 9), is also trivial. Indeed, with an increase in the thickness of a layer that conducts water, heat, electricity, and contaminants (according to the Darcy, Fourier, Ohm, Fick, and other resistivity laws), the flux of a corresponding substance always decreases if a layer is thickened, provided boundary conditions of a flow tube are kept (see Goldshteĭn & Entov, 1994; Polubarinova-Kochina, 1962). The theoretical support of a monotonic decrease of q with B at a constant D can be inferred from Gardner (1958), who considered the upper mulch layer to be a purely vapor conducting entity.

Willis (1960) extended Gardner's work and conducted an approximate theoretical analysis of steady evaporation (using the G-A equation) through a two-layered soil identical to that in our Figure 1. From Willis' Figure 8, for example, for $D = 200$ cm, one can already determine the nonmonotonic dependence of evaporation losses on the mulch thickness (our B), although the five Willis' curves at this D are cluttered. Figure 9 of Willis (1960) presents the results of column experiments that also indicate the nonmonotonicity of $q(B)$ at a fixed D. However, Willis did not systematically solve the problem of detecting the value of B that delivers an extremum of q. That would require a continuous variation of B (or, in Willis' vernacular, the position of the water table). Willis' experiment also manifests that at fixed B and D the flux q depends on the textural composition of his layered columns in a rather non-trivial manner.

In the field and lab experiments, agronomist and hydrologists found (see, e.g., Assouline et al., 2014; Ehlers & Van Der Ploeg, 1976; Jalota & Prihar, 1990; Klocke et al., 2009; Larson et al., 1983; Price et al., 1998; Prihar et al., 1996; Schwartz et al., 2010; Unger & Cassel, 1991; Willis & Bond, 1971; Wuest & Schillinger, 2011) that the layering of soil (by mulching, harrowing, spudding, tillage, machine-induced compaction, and by natural crust-seal formation) may both decrease and increase evaporation, which is apparently at odds with Gardner (1958).

We will now prove that the simplest possible Gardner (1958) model based on the 1-D, steady Richards' equation (ignoring, for example, vapor flow, transiency, intermittency with infiltration and redistribution, and moisture interception by plant roots), can explain the above-cited seemingly recalcitrant and incongruous results. Namely, we illustrate that $q(B)$ can be a single-extremum function for the flow sketched in Figure 1. The nonmonotonic function $q(B)$ corroborates the positive, negative, or no-impact of soil layering on evaporation.

We utilize modern computer algebra to solve ordinary differential equations (ODEs) and nonlinear equations involving numerical integrations (special functions), which Bakr et al. (1979), Gardner (1958), Gardner and Fireman (1958), Ripple et al. (1970), Salvucci (1993), Shi et al. (2014), Warrick (1988), Warrick and Yeh (1990), and Willis (1960), among others, faced when analytically studying evaporation through homogeneous and layered soils. In a sense, we have realized the program of Hillel et al. (1975), who, after numerical simulations of two-layered soils, stated the necessity to optimize heterogeneity of soils, in particular, mulching parameters (see also Al-Maktoumi et al., 2014; Betti et al., 2016). Along with the determination of the extrema of $q(B)$ for a two-layered composite in Figure 1 (with a G-E or G-A constituting relation in both layers), we extend our analysis to continuously heterogeneous soils.

2.1. G-E Conductivity Model for Two-Layered Soils

To be consistent with Philip's (1969, 1991) conventions, in this section, the direction of the vertical axis OZ is positive downward, with the origin O at the soil surface. We assume that both soil layers in Figure 1 are characterized by the dyads of the saturated hydraulic conductivity and the sorptive number (both are positive constants within each layer), (K_1,α_1) and (K_2,α_2), which are routinely determined in the lab (see, e.g., Wendroth & Wypler, 2008) or field (e.g., by tension infiltrometry), as well as from pedotransfer functions or stochastic models (e.g., Lu & Zhang, 2004). The unsaturated conductivities obey the relations

$$k_1(p_1) = K_1 \exp[\alpha_1\, p_1], \quad k_2(p_2) = K_2 \exp[\alpha_2\, p_2], \tag{1}$$

where $p_1(z)$ and $p_2(z)$ are the pressure heads (negative) in the corresponding layers of Figure 1.

The Darcy law states that

$$v_{1Z} = -k_1(p_1)\frac{\mathrm{d}p_1}{\mathrm{d}Z} + k_1(p_1), \quad v_{2Z} = -k_2(p_2)\frac{\mathrm{d}p_2}{\mathrm{d}Z} + k_2(p_2), \tag{2}$$

where $v_{1Z} = v_{2Z} = q$ are Philip's notations for the vertical Darcian velocities. Ripple et al. (1970, p.34) gave a hydrological balance rather than an agronomist's perspective of evaporation through stratified soils: "Often, the only information sought is the dependence of the soil-limited evaporation, upon the water table depth." We will also focus on q.

Along the interface M_1M_2, the continuities of pressure and flux require that $p_1 = p_2$ and $v_{1Z} = v_{2Z} = q = \text{const}$.

Following Philip, we introduce the Kirchhoff potentials in the two layers:

$$\phi_1 = \int_{-\infty}^{p_1} k_1(\mathrm{u})\mathrm{d}u = \frac{k_1(p_1)}{\alpha_1}, \quad \phi_2 = \int_{-\infty}^{p_2} k_2(\mathrm{u})\mathrm{d}u = \frac{k_2(p_2)}{\alpha_2}. \tag{3}$$

From the conservation of mass, we have two linear ODEs:

$$\begin{aligned} &\frac{\mathrm{d}^2\phi_1}{\mathrm{d}Z^2} - \alpha_1\frac{\mathrm{d}\phi_1}{\mathrm{d}Z} = 0, \quad B < Z < D, \\ &\frac{\mathrm{d}^2\phi_2}{\mathrm{d}Z^2} - \alpha_2\frac{\mathrm{d}\phi_2}{\mathrm{d}Z} = 0, \quad 0 < Z < B. \end{aligned} \tag{4}$$

The Kirchhoff potential is not continuous across M_1M_2; from the continuities of pressure and flux along this line, we obtain two equations,

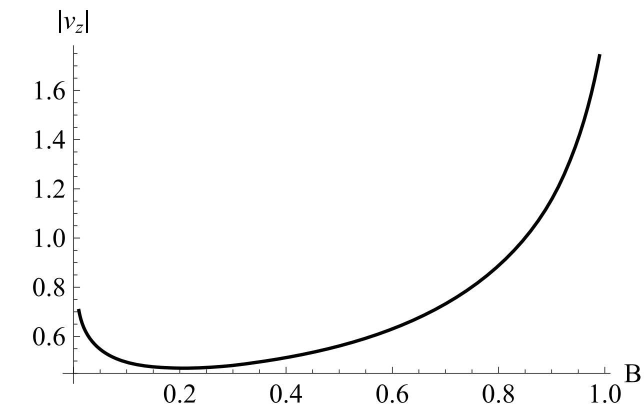

Figure 2. Gardner's exponential soils; an absolute value of the dimensionless evaporative flux $|v_z|$ as a function of B for a coarser upper layer: $K_2 = 100$, $\alpha_2 = 4$, $\alpha_1 = 0.4$, and $\phi_{2s} = 0$.

$$\frac{1}{\alpha_1}\ln\frac{\alpha_1\phi_1(B)}{K_1} = \frac{1}{\alpha_2}\ln\frac{\alpha_2\phi_2(B)}{K_2}, \quad \alpha_2\phi_2(B) - \frac{d\phi_2(B)}{dZ} = \alpha_1\phi_1(B) - \frac{d\phi_1(B)}{dZ}, \tag{5}$$

which serve for the determination of $\phi_1(B)$ and $\phi_2(B)$. We introduce dimensionless values: $Z^* = Z/D$, $B^* = B/D$, $a_1^* = a_1 D$, $a_2^* = a_2 D$, $K_2^* = K_2/K_1$, $p_1^* = p_1/D$, $p_2^* = p_2/D$, $\phi_1^* = \phi_1/(K_1 D)$, $\phi_2^* = \phi_2/(K_1 D)$, $\phi_{2s}^* = \phi_{2s}/(K_1 D)$, and $q^* = q/K_1$, which are slightly different from commonly used by Philip, Raats, Warrick, and others (see e.g., Blunt, 2017; Warrick, 2003) because we vary the capillary properties of the layers keeping D constant. We will drop "*" for the dimensionless quantities.

First, we solve two BVPs for equation (4) with the corresponding boundary conditions $\phi_1(1) = 1/\alpha_1$, $\phi_2(0) = \phi_{2s}$, and $p_1(B) = p_2(B)$:

$$\begin{aligned} \phi_1 &= \frac{\exp(\alpha_1 Z) - \exp(\alpha_1 B) + \alpha_1\phi_1(B)[\exp(\alpha_1) - \exp(\alpha_1 Z)]}{\alpha_1[\exp(\alpha_1) - \exp(\alpha_1 B)]}, \quad B < Z < 1, \\ \phi_2 &= \frac{[\exp(\alpha_2 Z) - 1]\phi_2(B) + \phi_{2s}[\exp(\alpha_2 B) - \exp(\alpha_2 Z)]}{\exp(\alpha_2 B) - 1}, \quad 0 < Z < B. \end{aligned} \tag{6}$$

From equation (6) we determine the flux:

$$\begin{aligned} q &= \alpha_1\phi_1 - \frac{d\phi_1}{dZ} = \frac{\alpha_1\phi_1(\mathrm{B})\exp(\alpha_1) - \exp(\alpha_1 B)}{\exp(\alpha_1) - \exp(\alpha_1 B)}, \quad B < Z < 1, \\ q &= \alpha_2\phi_2 - \frac{d\phi_2}{dZ} = \frac{\alpha_2[\phi_{2s}\exp(\alpha_2 B) - \phi_2(B)]}{\exp(\alpha_2 B) - 1}, \quad 0 < Z < B. \end{aligned} \tag{7}$$

From equations (5) and (7) we obtain

$$\phi_2(B) = \phi_{2s}\exp(\alpha_2 B) + \frac{\exp(\alpha_2 B) - 1}{\exp[\alpha_1(B-1)] - 1}\frac{\alpha_1\phi_1(B) - \exp[\alpha_1(B-1)]}{\alpha_2}. \tag{8}$$

Substituting (8) into the right-hand side of the first equation (5) we obtain a nonlinear equation with respect to $\phi_1(B)$. This equation is solved by the **FindRoot** routine in Wolfram's *Mathematica*. We placed the found root back into the first equation (7) and obtained the flux v_{1Z} as a function of (K,α), that is, of hydraulic-capillary properties of the two soils, thickness B, and the potential at the soil surface ϕ_{2s} (a constant determined by the atmospheric conditions).

Figure 2 shows the modulus $|v_z|$ as a function of B for a mulch material with $K_2 = 100$, $\alpha_2 = 4$, $\alpha_1 = 0.4$ and an absolutely dry soil surface S_1S_2 that corresponds to $\phi_{2s} = 0$. In prescribing this boundary condition at the soil surface, we followed Philip (1991). He also assumed that the soil surface is absolutely dry that gave the *upper bound* of evaporation losses. Physically, evaporation through a very dry soil is prevalently in a vapor form, with a minor contribution of liquid motion through corner zones of pore channels, which Blunt (2017) modeled as triangles. Philip (1991) still used Richards' equation in domains with a dry-soil boundary condition.

The minimum of $|v_z|$, $q_m = 0.47$, is attained at $B_m = 0.21$. The minimum in Figure 2 is quite pronounced. Similarly, optimal Bs were obtained for other K_2, α_2, α_1 of the G-E model.

Figure 3 shows $|v_z|$ as a function of B of the topsoil, which is less permeable and has higher capillarity than the substratum: $K_2 = 0.5$, $\alpha_2 = 4$,

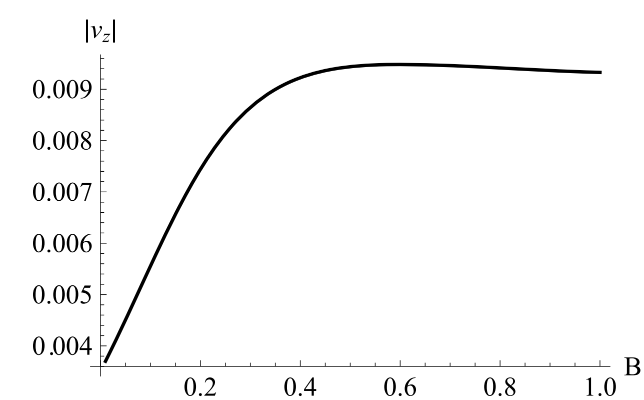

Figure 3. Gardner's exponential soils; an absolute value of the dimensionless evaporative flux $|v_z|$ as a function of B for a finer upper layer: $K_2 = 0.5$, $\alpha_2 = 4$, $\alpha_1 = 4\sqrt{2}$, and $\phi_{2s} = 0$.

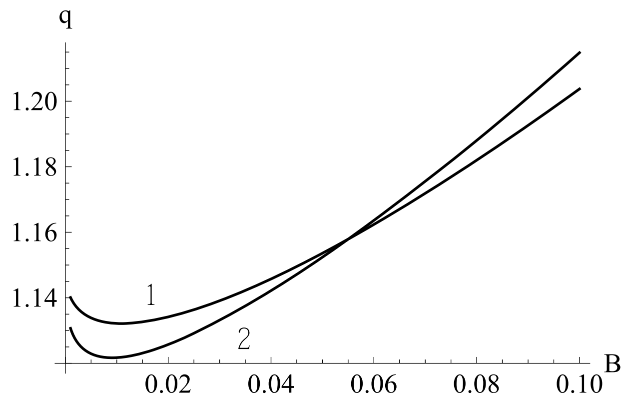

Figure 4. Gardner's algebraic soils; dimensionless $q(B)$ for $D = 20$ cm. Layer 1 is Yolo clay: $n_1 = 2$, $a_1 = 400$ cm^3/day, $b_1 = 400$ cm^2, and $K_1 = 1$ cm/day, and layer 2 is Pachapa sandy loam: $n_2 = 3$, $a_2 = 3.2 \cdot 10^5$ cm^4/day, $b_2 = 2.6 \cdot 10^4$ cm^3, and $K_2 = 12.3$ cm/day (curve 1). Layer 1 is Yolo clay, and layer 2 is Willis' sand: $n_2 = 4$, $a_2 = 1.7 \cdot 10^8$ cm^4/day, $b_2 = 2.6 \cdot 10^6$ cm^3, and $K_2 = 68$ cm/day (curve 2). The soil surface is extremely dry.

$\alpha_1 = 4\sqrt{2}$, and $\phi_{2s} = 0$. For this composite, the magnitude of the flux attains a maximum, q_M = 0.0095, at B_M = 0.6. The minimum, q_m = 0.0035, is attained at B_m = 0. Consequently, in this case, the fine top layer of any thickness (e.g., created by the above-mentioned soil crusting) would evaporationally spoil a coarse homogeneous background soil. This is contrary to what Ripple et al. (1970) found for a two-layered (crusted) soil: "… a relatively thin less permeable layer may markedly decrease evaporation rates" (see their Figure 9). In Ripple's Figure 9, the curves for q at small B (in our notation) for two-layered soils are indistinguishable from those of a homogeneous soil. That may be caused by an insufficient accuracy of Ripple's iterative solutions of the nonlinear equations. Indeed, half a century ago, before the advent of computer algebra, it would not have been easy to detect the extrema in our Figures 2 and 3.

We note that Kumar (1999) also found minima of the function $|v_z(B)|$ for a coarse upper stratum, as in our Figure 1. However, Kumar's computations were cumbersomely indirect; he numerically (using a finite difference method) solved a transient Richards' equation and considered a steady-state limit with the same boundary conditions as in our analytic solution. He obtained that limit for a few values of B. In our computer algebra code, the $q(B)$ curves and extrema on them are found in a trice.

2.2. G-A Conductivity Model for a Two-Layered Soil

In this section, we select algebraic functions rather than *G-E* equation (1):

$$k_1(S_1) = \frac{a_1}{S_1^{n_1} + b_1} = \frac{K_1}{S_1^{n_1}/b_1 + 1}, \quad k_2(S_2) = \frac{a_2}{S_2^{n_2} + b_2} = \frac{K_2}{S_2^{n_2}/b_2 + 1}, \tag{9}$$

where, for consistency with Gardner-Warrick's notations, we use the suction pressure heads $S_{1,2} = -p_{1,2}$ and a vertical coordinate OZ_G, with an origin at the water table (Figure 1). This axis is oriented upward such that $q = v_z$ is now co-oriented with OZ_G. In equation (9), the triads ($a_{1,2}$, $b_{1,2}$, and $n_{1,2}$) are composed of mathematically arbitrary positive constants that characterize the two soil layers in Figure 1. Equation (2), with (9) inserted, separate and are integrated as

$$\begin{aligned} Z_G &= \int_0^{S_1} \frac{du}{q/k_1(u) + 1}, \quad 0 < Z_G < D{-}B, \quad 0 < S_1 < S_{2B}, \\ Z_G &= \int_{S_{2B}}^{S_2} \frac{du}{q/k_2(u) + 1}, \quad D{-}B < Z_G < D, \quad S_{2B} < S_2 < S_S. \end{aligned} \tag{10}$$

Obviously, $S_{2b} = S_{1b}$ (the suction at the interface is continuous). This constant, as well as q, must be found.

We introduce dimensionless values $Z_G^* = Z_G/D, B^* = B/D, S_1^* = S_1/D, S_2^* = S_2/D, b_1^* = b_1/D^2, b_2^* = b_2/D^2$, $q^* = q/K_1$, and $K_2^* = K_2/K_1$, and drop the "*". Equation (10) is then integrated by the **Integrate** routine in Wolfram's (1991) *Mathematica* as

$$\begin{aligned} &Z_G(S_1) = \frac{S_1}{1+q} F\left[1, 1/n_1; 1 + 1/n_1; -\frac{qS_1^{n_1}}{b_1 + b_1 q}\right], \quad 0 < Z_G < 1 - B, \quad 0 < S_1 < S_{1B}, \\ &Z_G(S_2) = 1{-}B + \frac{K_2}{K_2 + q}\left(S_2 F\left[1, \frac{1}{n_2}; 1 + \frac{1}{n_2}; \frac{-qS_2^{n_2}}{b_2(K_2+q)}\right] - S_{1B} F\left[1, \frac{1}{n_2}; 1 + \frac{1}{n_2}; \frac{-qS_{1B}^{n_2}}{b_2(K_2+q)}\right]\right), \\ &1{-}B < Z_G < 1, \quad S_{2B} < S_2 < S_S, \end{aligned} \tag{11}$$

where F is the hypergeometric function ${}_2F_1$.

Since Gardner (1958), (We recall that Gardner himself generalized the earlier Wind and Remson-Fox empirical $k(S)$ functions.) soil scientists have studied approximate solutions of equation (10) and exact solutions for various special cases of the G-A function, for example, $n = 1, 3/2, 2, 3$, and 4, for which the integrals

10.1029/2018WR024025

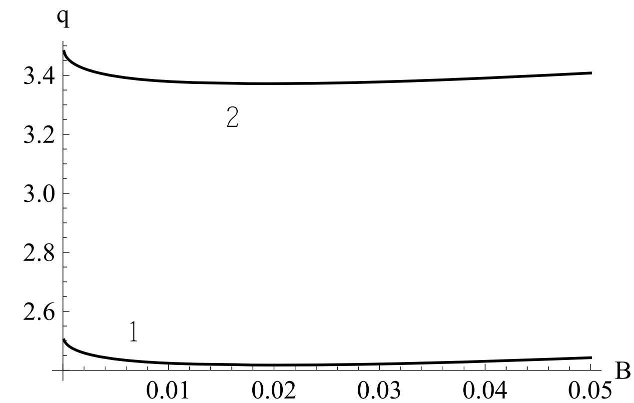

Figure 5. Gardner's algebraic soils; layer 1 is Diablo loam: $n_1 = 2$, $a_1 = 700$ cm^3/day, $b_1 = 1450$ cm^2, and $K_1 = 0.48$ cm/day, and layer 2 is Willis' sand. Dimensionless $q(B)$ for $D = 20$ cm (curve 1) and $D = 15$ cm (curve 2). The soil surface is extremely dry.

in (10) are evaluated in arctan-log functions. These quadratures were subject to several inversions $Z_G(S) \to S(Z_G)$ in expression (11); e.g., see Bakr et al., 1979; Ripple et al., 1970; Salvucci, 1993; Shi et al., 2014; Warrick, 1988). Using *Mathematica*, a systematic solution of nonlinear equations involving special functions and a continuous variation of all involved parameters (n, a, and b in (9) and S_s, B, and D in the BVP for an ODE) is a standard procedure for any n. Consequently, we set $S_1 = S_{1\mathrm{B}}$ and $Z_G = 1\text{-}B$ and $S_2 = S_s$ and $Z_G = 1$ in the corresponding first and second equations (11). We solved the obtained system of two nonlinear equations with respect to the pair ($S_{1\mathrm{B}}$, q) using the *Mathematica* **FindRoot** routine (We recall that at $n_1 = n_2 = 2$ for the clay-like layers in Figure 1, the suction head S_{1B} along the interface is explicitly expressed through q, and the system (11) is simplified to one nonlinear equation with respect to q, analogous to the case of the G-E functions from section 2.1.).

2.2.1. Examples

We first consider $D = 20$ cm and use the Gardner and Fireman (1958) data for soil properties; layers 1 and 2 in Figure 1 are Yolo clay and Pachapa sandy loam, for which the corresponding dimensional parameters in equation (9) are $n_1 = 2$ and $a_1 = 400$ cm^3/day, $b_1 = 400$ cm^2, and $K_1 = 1$ cm/day, and $n_2 = 3$, $a_2 = 3.2 \cdot 10^5$ cm^4/day, $b_2 = 2.6 \cdot 10^4$ cm^3, and $K_2 = 12.3$ cm/day.

In Figure 4, curve 1 shows the corresponding dimensionless evaporation losses $q(B)$. Next, we used the same D and Yolo clay of layer 1 for layer 2. Instead of the Pachapa soil, we used the river bed sand from Willis (1960), for which $n_2 = 4$, $a_2 = 1.7 \cdot 10^8$ cm^4/day, $b_2 = 2.6 \cdot 10^6$ cm^3, and $K_2 = 68$ cm/day. The losses for this two-layered composite are shown as curve 2 in Figure 4.

It is evident from Figure 4 that evaporation is indeed reduced by a thin (approximately 1 cm) layer of a coarser material placed on the top of the Yolo clay. In addition, we have a mild minimum of $q(B)$ for both two-layered soils. This minimum can easily go unnoticed in experiments. At a given B and D, a coarser mulch (Willis' sand in Figure 4) may—depending on B—evaporate less (at $B < B_i$) or more (at $B > B_i$) than a finer mulch (Pachapa's sandy loam) with the same thickness B. The two curves in Figure 4 intersect at $B = B_i = 0.05$. We recall that Yuan et al. (2009) also varied the mulch properties and found in their drying experiments that the finest mulch evaporated less than coarser ones.

In the second example, layer 1 is the Diablo loam from Willis (1960), for which $n_1 = 2$, $a_1 = 700$ cm^3/day, $b_1 = 1450$ cm^2, and $K_1 = 0.48$ cm/day, and layer 2 is Willis' riverbed sand. We varied D from 20 to 15 cm. The corresponding curves of $q(B)$ are shown as curves 1 and 2 in Figure 5. Again, as in Figure 4, both curves in Figure 5 have minima (we computed the minima using the **FindMinimum** *Mathematica* routine) at approximately the same dimensionless $\underline{B_{\mathrm{m}}} = 0.02$. The minimum q_{m} increased significantly (from 2.4 to 3.4) with an decrease in D. We recall Hadas' (1997) conclusion: "Tillage-produced 'soil mulch,' a structured soil layer, reduces soil water evaporation in a similar manner to plant residues mulch, provided its aggregate sizes range between 8.3 and 5.0 mm diameter and its depth is between 5 and 10 cm."

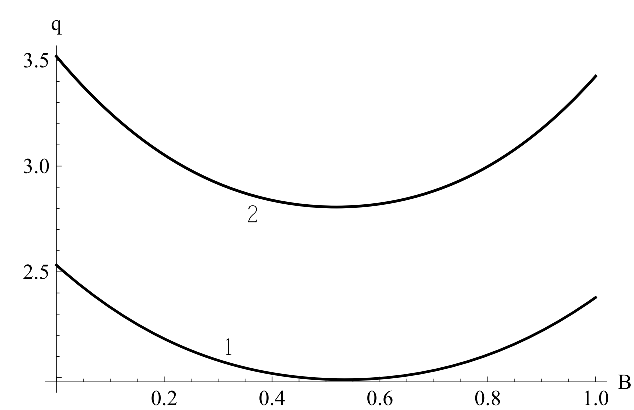

Figure 6. Gardners' algebraic soils; layer 1 is Diablo loam; layer 2 is Yolo clay. Dimensionless $q(B)$ at $D = 20$ cm (curve 1) and $D = 15$ cm (curve 2). The soil surface is extremely dry.

In the third example, we selected two claylike layers, the Diablo and Yolo soils, as layers 1 and 2. In Figure 6, curves 1 and 2 show $q(B)$ at $D = 20$ cm and 15 cm, respectively. In comparison with Figure 5, much more pronounced minima were attained at $B_{\mathrm{m}} = 0.54$ and 0.52.

In the fourth example, a homogeneous Diablo clay with $D_0 = 48$ cm had $q_0 = 0.84$. The subscript here indicates the soil which is either *thickened* or heterogenized in the following manner. We compared two types of melioration of D_0: thin mulching with the addition of Willis' sand of thickness $B = 2$ cm on the top of the clay (making $D = 50$ cm) and hallowing, which converted a layer of thickness $B = 10$ cm into a pseudo-Yolo clay

10.1029/2018WR024025

(retaining $D = 48$ cm). From equation ((11)) we get for the former $q_1 = 0.7$ and for the latter $q_2 = 0.74$, these composites reduce evaporative losses by approximately 17 and 12%, respectively, compared with a homogeneous soil.

2.3. Average Suction in the Composite

The distributions $S(Z)$ in Figure 1 can be immediately obtained by inverting equation (11) using *Mathematica* routines. Here we introduce the vertically averaged values of the capillary pressure head in the strata of Figure 1:

$$CP_1 = \frac{1}{1-B}\int_0^{1-B} S_1(Z_G)\mathrm{d}Z_G, \quad CP_2 = \frac{1}{B}\int_{1-B}^{1} S_2(Z_G)\mathrm{d}Z_G, \quad CP = CP_1 + CP_2 \tag{12}$$

We computed the integrals in (12). For the example of the Diablo-Yolo clay ($D = 20$ cm, curve 1 in Figure 6), $CP_m = 34.8$ for the minimal-q composite.

2.4. Continuous Variation in Soil Properties With Depth

Do the minima for q occur in soils with continuous variations in hydraulic properties with Z? In this section, we return to the G-E model and Philip's vertical coordinate convention in Figure 1. Now we assume that $k(Z) = K_0(Z)\exp[\alpha(Z)\, p(Z)]$, where $K_0(Z)$ and $\alpha(Z)$ are two given functions. For simplicity, we assume that these two functions are correlated according to an empirical function from Communar and Friedman (2015):

$$\alpha(Z_G) = C_a\sqrt{K_0(Z)}, \tag{13}$$

where $K_0(Z)$ is in cm/hr, $\alpha(Z)$ is in 1/cm, and C_a is in $\mathrm{h}^{1/2}/\mathrm{cm}^{3/2}$. There are numerous pedotransfer functions and other empirical relations between $K_0(Z)$ and $\alpha(Z)$, which can be used instead of equation (13). For arbitrary $K_0(Z)$ and $\alpha(Z)$ in equation (13), the first-order ODEs (2) cannot be integrated in the form of $Z(p)$ as in Gardner (1958), Willis (1960), and Warrick (1988). Instead, we must numerically solve a BVP for an ODE (e.g., see Salvucci, 1993):

$$\frac{\mathrm{d}p(Z)}{\mathrm{d}Z} + \frac{v_Z}{K_0(Z)}\exp\left[-C_a\sqrt{K_0(Z)}p(Z)\right] - 1 = 0, \qquad 0 < Z < D, \quad p(0) = p_s, \quad p(D) = 0. \tag{14}$$

This is easily done using the *Mathematica* **NDSolve** routine, but integration in quadratures is not possible.

There is still some room for explicit integration of (14) if we expand the exponent there into a Taylor series and retain the first two terms (also see Barontini et al., 2007, for a similar linearization of Richards' equation with the G-E $k(S)$ in transient evaporation models). This linearization reduces (14) to a linear ODE:

$$\frac{\mathrm{d}p(Z)}{\mathrm{d}Z} - \frac{C_a v_Z}{\sqrt{K_0(Z)}}p(\mathrm{Z}) = 1 - \frac{v_Z}{K_0(Z)}, \qquad 0<Z<D, \quad p(0) = p_s, \quad p(D) = 0. \tag{15}$$

A general solution of BVP (15) is

$$p(\mathrm{Z}) = \exp\left(C_a v_Z\int_0^Z \frac{\mathrm{d}t}{\sqrt{K_0(t)}}\right)\left(c + \int_0^Z\left(1 - \frac{v_Z}{K_0(t)}\right)\exp\left(-C_a v_Z\int_0^t \frac{\mathrm{d}\tau}{\sqrt{K_0(\tau)}}\right)\mathrm{d}t\right). \tag{16}$$

The constant of integration $c = p_s$ here is due to the boundary condition at $Z = 0$. Using the boundary condition at $Z = D$ in (15), we obtain the following nonlinear equation with respect to v_Z:

$$\int_0^D\left(1 - \frac{v_Z}{K_0(t)}\right)\exp\left(-C_a v_Z\int_0^t \frac{\mathrm{d}\tau}{\sqrt{K_0(\tau)}}\right)\mathrm{d}t = -p_S. \tag{17}$$

For a given particular $K_0(z)$, we can reduce a nonlinear integral equation (17) to an algebraic one. For example, if

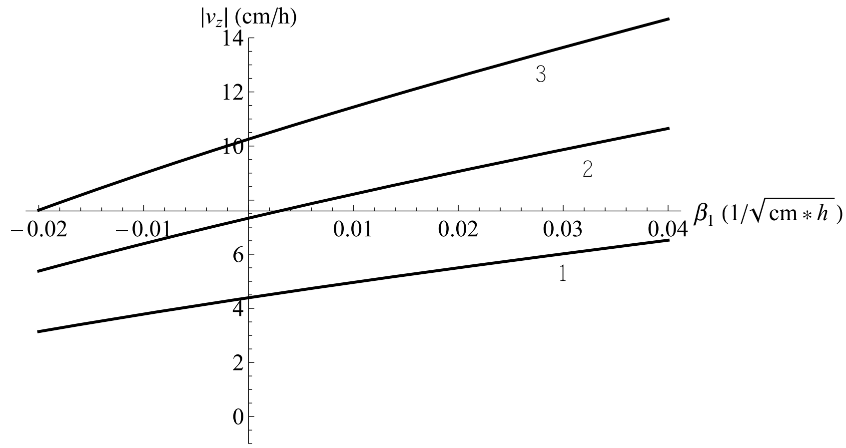

Figure 7. Dimensional evaporation losses as a function of β_1 for Gardner's exponential unsaturated conductivity function. The saturated hydraulic conductivity K_0 varies with Z according to equation (18); the sorptive number is correlated to K_0 according to (13). Curves 1–3 correspond to three values of suction, $p_s = -1{,}000$, $-10{,}000$, and $-100{,}000$ cm (curves 1–3, respectively).

$$K_0(\mathrm{Z}) = (\beta_1 Z + \beta_2)^2 \quad (\beta_1 Z + \beta_2 \neq 0, \quad \forall Z \in [0, D]), \tag{18}$$

we get

$$\left(\frac{\beta_2}{\beta_1 - C_a v_z} + \frac{v_z/\beta_2}{\beta_1 + C_a v_z} - p_S\right)\left(\frac{\beta_1 D + \beta_2}{\beta_2}\right)^{C_a v_z/\beta_1} = \frac{\beta_1 D + \beta_2}{\beta_1 - C_a v_z} + \frac{v_z/(\beta_1 D + \beta_2)}{\beta_1 + C_a v_z}. \tag{19}$$

We used the **FindRoot** routine in *Mathematica* to solve equation (19) with respect to v_z.

Figure 7 shows the magnitude of the dimensional evaporative flux in cm/hr as a function of β_1 at $D = 20$ cm, $\beta_2 = 1$ (cm/hr)$^{1/2}$, and $C_a = 0.04$ h$^{1/2}$/cm$^{3/2}$ for three values of suction, $p_s = -1{,}000$, $-10{,}000$, and $-100{,}000$ cm (curves 1–3, respectively).

If we retain the third (quadratic) term in the Taylor series expansion of the exponential function in (14), then the BVP for the nonlinear ODE is

$$\frac{\mathrm{d}p(Z)}{\mathrm{d}Z} - v_Z\left(\frac{0.04}{\sqrt{K_0(Z)}}p(Z) + 0.0008p(Z)^2 + \frac{1}{K_0(Z)}\right) - 1 = 0, \quad 0 < \mathrm{Z} < D, \quad p(0) = p_s, \quad p(\mathrm{D}) = 0. \tag{20}$$

We solved (20) using the **NDSolve** *Mathematica* routine in the same manner as the nonlinearized BVP (14). It is noteworthy that **NDSolve** and **FindRoot** use numerical evaluations (see Wolfram, 1991) for integration and root finding, which fail if the initial guesses are poor (we skip over examples of such types of crashes for the routines in our computations).

3. HYDRUS-1D Simulations

In this section, we use HYDRUS-1D (Šimůnek et al., 2016), a public domain software that solves the governing water flow (Richards) equation using the finite element method. In all transient flow simulations, time, t, is in days and the vertical size of two-layered columns is in centimeter. We use several default HYDRUS options: no vapor flow, the VGM capillary pressure and phase permeability functions, and the HYDRUS Soil Catalogue.

The column in Figure 1 is composed of clay (stratum 1) and sand (stratum 2).

As in the analytical solution of section 2 we fixed the total thickness $D = 20$ cm (HYDRUS-1D works with dimensional quantities). An finite element mesh discretizes it into 500 elements in the vertical, Z_H, direction. The bottom and top boundary conditions are constant pressure heads $p = 0$ and $p_s = -10{,}000$ cm,

10.1029/2018WR024025

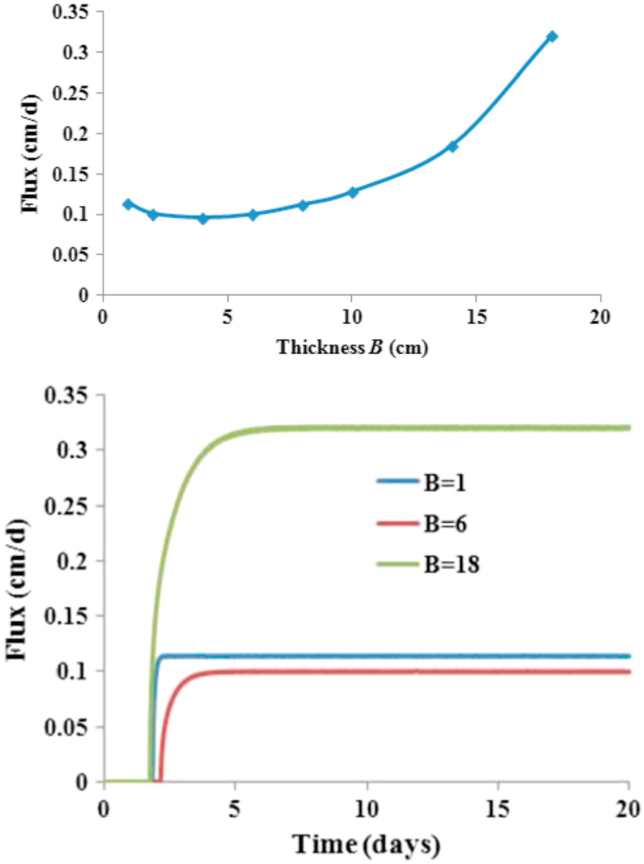

Figure 8. (top) The dimensional steady-state evaporation rate (flux) as a function of the thickness B and (bottom) the transient evaporation rates for thicknesses $B = 1$, 6, and 18 cm. The evaporation rate is calculated using HYDRUS-1D from an isobar $p = -10{,}000$ cm, S_1S_2 (Figure 1) for a two-layered soil of the total thickness $D = 20$ cm, and varying thickness B of the top mulch made of a coarse layer (sand) with a subjacent clay layer and water supply from an isobar $p = 0$ cm, W_1 W_2.

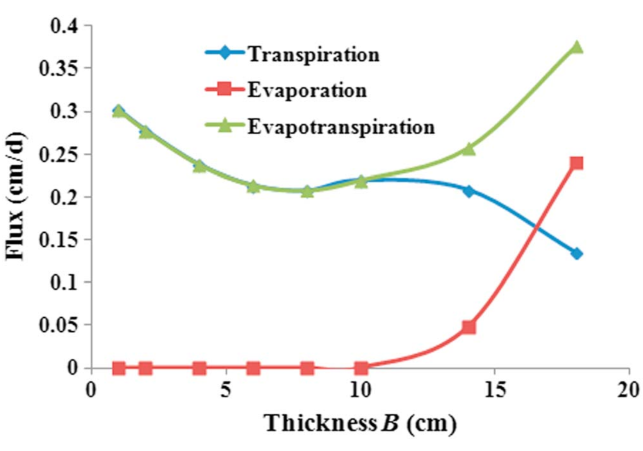

Figure 9. Dimensional steady-state evaporation fluxes as functions of B for the same composite as in Figure 8 but root water uptake by Feddes' grass added in HYDRUS simulations: total evapotranspiration, evaporation, and transpiration.

respectively. Initially, the pressure head is distributed hydrostatically between these two values. Simulations are run for t = 20 days during which steady-state evaporation from the water table is established. Because of the very steep retention curve of the default sand, when small changes in the water content correspond with large changes in the pressure head (for sands the pressure head can fluctuate from −100 to −10,000 while still being within the default HYDRUS-1D water content tolerance limit of 0.001), the water content tolerance was reduced to 1.e −5. We also disabled the internal interpolation tables to get more precise results. The steady-state and transient surface fluxes at the top of the soil column computed using HYDRUS-1D are plotted in Figure 8 as a function of the thickness B (top) and for three values of $B = 1$, 6, and 18 cm (bottom), respectively. In notations of Figure 2, the results are $|v_z| = 0.114$, 0.1003, and 0.320 cm/day. Therefore, at the mulch thickness $B = 6$ cm a minimum (actually, a pseudo-minimum for these three discrete values of B) is attained. We surmise that the minimum is unique, global, and close to the pseudo-minimum. Thus, the analytically found extremum in Figure 2 for Gardner's bare soils and finite difference method extrema found by Kumar (1999) are qualitatively corroborated by FEM simulations for VGM two-component composites.

The effect of uptake by plants' roots on water flow and the water content distribution along the unsaturated soil profile often prevails over a purely capillary flow. In order to quantify this juxtaposition of evaporation, transpiration, and variation of the thickness of our composite we used the root water uptake (RWU) model in HYDRUS-1D, assuming a grass with a uniform root distribution throughout the profile ($0 < Z_G < 20$ cm in Figure 1), Feddes' stress response function, and potential transpiration of 0.5 cm/day. The results are shown in Figure 9 (for discretely varied $B = 2, 4, \ldots 16, 18$ cm) and evidence the following. The total evapotranspirative flux still has a global minimum with B as for pure evaporation.

For small thicknesses of sand, there is no evaporation and only RWU declining with the sand thickness. Once the profile is mostly sand (14–18 cm), there is a further reduction in RWU, while the profile starts evaporating. It is noteworthy that the RWU curve in Figure 9 exhibits a startling, hardly expected behavior: a global end-maximum at $B = 2$ cm, a global end-minimum at $B = 18$ cm, and two internal extrema, viz., local maximum and minimum.

4. Concluding Remarks

We examined a 1-D ascending flow through an unsaturated two-layered soil in Figure 1. Analytically, we did not study soils' transient multistage drying but rather analyzed a steady-state evaporation from a stationary isobar (water table), as Gardner, Willis, and Warrick did. For each stratum in Figure 1, we used the Gardner (1958) exponential and algebraic functions for the unsaturated conductivity-suction pressure head $k(S)$, which are characterized by dyads and triads of empirical soils' constants. We employed modern computer algebra routines (solutions of systems of nonlinear equations, integration, finding minima, and evaluation of hypergeometric functions) to determine the constant evaporation flux q as a function of the thickness B of the upper stratum of the unsaturated zone. We interpreted this texturally contrasted stratum as mulching/tillage and illustrated that $q(B)$ might have nontrivial minima

(q_m, B_m) if the total composite thickness D is fixed, a fact found numerically by Kumar (1999). Numerical simulations in HYDRUS-1D for the van Genuchten soil properties qualitatively corroborate the analytical results, viz., for a fixed total thickness of a two-layered soil a certain thickness of the upper coarse layer minimizes an evaporative flux from bottom isobar to a top one. A HYDRUS-simulated example with Feddes' grass uptaking moisture from the soil composite illustrates nontrivial extrema of the global flux from a shallow water table and of the transpiration due to water uptake by plants' roots.

The reduction in q by shallow (1–2 inches of B in Figure 1) spudding/harrowing (without traditional tillage) was tested by Ovsinsky (1899) and later replicated and developed for various climatic and agronomic conditions (Allen, 1981; Faulkner, 1943; Friedrich et al., 2014; Kassam et al., 2018; Maltsev, 1954; Novakovska et al., 2018; Verhulst et al., 2010; Yadav et al., 2018). Along with many other advantages (including a better aeration of the root zone, circadian condensation of the dew in the B-layer of Figure 1, better nitrification and ensued reduction or the elimination of the application of agrochemicals, and more prolific activity of soil microbes), this no-till technology in semiarid climates preserves more moisture in the root zone. No-till or *shallow soil treatment* technology is, of course, not a panacea in agronomy (constraints and drawbacks are discussed, for example, by Garmashov, 2018; Pykhtin, 2017; and Turusov et al., 2018). Indeed, even if solely evaporation losses are a mathematical criterion, the minima in Figures 2 and 8 are rather *mild*, that is, even optimal mulching only moderately reduces the ascending flux.

Abbreviations

BVP	= boundary value problem
G-E	= Gardner's exponential unsaturated conductivity relation $k(S)$
G-A	= Gardner's algebraic function for unsaturated conductivity $k(S)$
ODE	= ordinary differential equation
PDE	= partial differential equation
VGM	= van Genuchten-Mualem

Acknowledgments
This work was funded by a grant from the Sultan Qaboos Higher Center for Culture and Science – Diwan of Royal Court and the Research Council of Oman (TRC) [RC/AGR/SWAE/17/01] and by the subsidy allocated to Kazan Federal University for the state assignment in the sphere of scientific activities, project1.12878.2018/12.1. Helpful comments by three anonymous referees are appreciated. The paper is theoretical, and no data are used.

References

Allen, H. P. (1981). *Direct drilling and reduced cultivation*. Ipswich: Farming Press.
Al-Maktoumi, A., Al-Ismaily, S., Kacimov, A., Al-Busaidi, H., Al-Saqri, S., & Al-Haddabi, M. (2014). Soil substrate as a cascade of capillary barriers for conserving water in a desert environment: Lessons learned from arid nature. *Journal of Arid Land*, *6*(6), 690–703. https://doi.org/10.1007/s40333-014-0068-7
Al-Shukaili, A., (2018). The effect of stratification on sand dunes hydrology in arid zone environments: Case of Oman. MSc dissertation. Sultan Qaboos University, Oman.
Assouline, S., Narkis, K., Gherabli, R., Lefort, P., & Prat, M. (2014). Analysis of the impact of surface layer properties on evaporation from porous systems using column experiments and modified definition of characteristic length. *Water Resources Research*, *50*, 3933–3955. https://doi.org/10.1002/2013WR014489
Bakr, H. M. A., Fathi, A. M., & Gheibeh, A. R. S. (1979). Evaluation of the parameters involved in Gardner's relation between unsaturated hydraulic conductivity and soil water matric suction. *Agricultural Water Management*, *2*(1), 25–35.
Barontini, S., Ranzi, R., & Bacchi, B. (2007). Water dynamics in a gradually nonhomogeneous soil described by the linearized Richards equation. *Water Resources Research*, *43*, W08411. https://doi.org/10.1029/2006WR005126
Betti, G., Grant, C. D., Murray, R. S., & Churchman, G. J. (2016). Size of subsoil clods affects soil-water availability in sand–clay mixtures. *Soil Research*, *54*(3), 276–290. https://doi.org/10.1071/SR15115
Blunt, M. J. (2017). *Multiphase flow in permeable media: A pore-scale perspective*. Cambridge: Cambridge University Press. https://doi.org/10.1017/9781316145098
Boast, C. W., & Simmons, F. W. (2005). Evaporation of water from bare soil. In D. Hillel (Ed.), *Encyclopedia of Soils in the Environment*, (pp. 494–502). Oxford: Elsevier. https://doi.org/10.1016/B0-12-348530-4/00358-1
Bodner, G., Nakhforoosh, A., & Kaul, H. P. (2015). Management of crop water under drought: A review. *Agronomy for Sustainable Development*, *35*(2), 401–442.
Communar, G., & Friedman, S. P. (2015). Cylindrically confined flows of water from a point source and to a sink, above a water table. *Vadose Zone Journal*, *14*(8). https://doi.org/10.2136/vzj2014.12.0183
Connolly, R. D. (1998). Modelling effects of soil structure on the water balance of soil–crop systems: A review. *Soil and Tillage Research*, *48*(1-2), 1–19. https://doi.org/10.1016/S0167-1987(98)00128-7
De Luca, D. L., & Cepeda, J. M. (2016). Procedure to obtain analytical solutions of one-dimensional Richards' equation for infiltration in two-layered soils. *Journal of Hydrologic Engineering*, *21*(7), 04016018.
Ehlers, W., & Van Der Ploeg, R. R. (1976). Evaporation, drainage and unsaturated hydraulic conductivity of tilled and untilled fallow soil. *Zeitschrift für Pflanzenernährung und Bodenkunde*, *139*(3), 373–386. https://doi.org/10.1002/jpln.19761390312
Faulkner, E. H. (1943). *Plowman's Folly*. Norman: Univ. of Oklahoma Press.

Felde, V. J. M. N. L., Peth, S., Uteau-Puschmann, D., Drahorad, S., & Felix-Henningsen, P. (2014). Soil microstructure as an under-explored feature of biological soil crust hydrological properties: Case study from the NW Negev Desert. *Biodiversity and Conservation*, *23*(7), 1687–1708. https://doi.org/10.1007/s10531-014-0693-7

Friedrich, T., Kassam, A., Corsi, S., Jat, R. A., Sahrawat, K. L., & Kassam, A. H. (2014). Conservation agriculture in Europe. In R. A. Jat, K. L. Sahrawat, & A. H. Kassam (Eds.), *Conservation agriculture: Global prospects and challenges* (pp. 127–170). Boston: CABI Press.

Fuchs, M., & Hadas, A. (2011). Mulch resistance to water vapor transport. *Agricultural Water Management*, *98*(6), 990–998. https://doi.org/10.1016/j.agwat.2011.01.008

Gardner, W. R. (1958). Some steady solutions of the unsaturated moisture flow equation with application to evaporation from a water table. *Soil Science*, *85*(4), 228–232. https://doi.org/10.1097/00010694-195804000-00006

Gardner, W. R., & Fireman, M. (1958). Laboratory studies of evaporation from soil columns in the presence of a water table. *Soil Science*, *85*(5), 244–249. https://doi.org/10.1097/00010694-195805000-00002

Garmashov, V. M. (2018). Principles and methods of optimization of basic soil treatment and rehabilitation of fertility of common chernozem by crop rotation in the Central Chernozem Zone. DSc. Dissertation, Kamennaya Step, Russia (in Russian).

Geng, X., & Boufadel, M. C. (2015). Numerical modeling of water flow and salt transport in bare saline soil subjected to evaporation. *Journal of Hydrology*, *524*, 427–438. https://doi.org/10.1016/j.jhydrol.2015.02.046

Goldshteĭn, R. V., & Entov, V. M. (1994). *Qualitative methods in continuum mechanics. Pitman monographs and surveys in pure and applied , athematics*, (Vol. 72). Harlow: Longman.

Hadas, A. (1997). Soil tilth—The desired soil structural state obtained through proper soil fragmentation and reorientation processes. *Soil and Tillage Research*, *43*(1-2), 7–40. https://doi.org/10.1016/S0167-1987(97)00033-0

Hillel, D., & Talpaz, H. (1977). Simulation of soil water dynamics in layered soils. *Soil Science*, *123*(1), 54–62. https://doi.org/10.1097/00010694-197701000-00007

Hillel, D. I., Van Bavel, C. H. M., & Talpaz, H. (1975). Dynamic simulation of water storage in fallow soil as affected by mulch of hydrophobic aggregates. *Soil Science Society of America Journal*, *39*(5), 826–833. https://doi.org/10.2136/sssaj1975.03615995003900050015x

Jalota, S. K., & Prihar, S. S. (1990). Bare-soil evaporation in relation to tillage. In B. A. Stewart (Ed.), *Advances in Soil Science*, (Vol. 12, pp. 187–216). New York: Springer.

Kacimov, A., & Obnosov, Y. V. (2018). Hydraulically optimal porous liner around a porous lens: Strack's problem revisited. *Journal of Hydraulic Engineering ISH*, 1–11. https://doi.org/10.1080/09715010.2018.1516576

Kassam, A., Friedrich, T. and Derpsch, R., 2018. *Global spread of conservation agriculture*. International J. of Environmental Studies, https://doi.org/10.1080/00207233.2018.1494927

Khan, A. R. (1988). Assessing the evaporation zone in the bare soil from the soil water flux and soil heat flux measurements. *Journal of Agronomy and Crop Science*, *161*(4), 234–237. https://doi.org/10.1111/j.1439-037X.1988.tb00662.x

Klocke, N. L., Currie, R. S., & Aiken, R. M. (2009). Soil water evaporation and crop residues. *Transactions of the ASABE*, *52*(1), 103–110. https://doi.org/10.13031/2013.25951

Kornev, V. G. (1935). *Subsurface irrigation*. Moscow-Leningrad: Selhozgiz. (in Russian)

Kumar, C. P. (1999). Evaporation from shallow water table through layered soil profiles. *ISH Journal of Hydraulic Engineering*, *5*(2), 65–75. https://doi.org/10.1080/09715010.1999.10514654

Larson, W. E., Swan, J. B., & Shaffer, M. J. (1983). Soil management for semiarid regions. *Agricultural Water Management*, *7*(1–3), 89–114. https://doi.org/10.1016/0378-3774(83)90077-X

Li, H., Wu, F., Zhan, H., Qiu, F., & Wang, W. (2016). The effect of precipitation pulses on evaporation of deeply buried phreatic water in extra-arid areas. *Vadose Zone Journal*, *15*(5). https://doi.org/10.2136/vzj2015.09.0127

Lu, Z., & Zhang, D. (2004). Analytical solutions to steady state unsaturated flow in layered, randomly heterogeneous soils via Kirchhoff transformation. *Advances in Water Resources*, *27*(8), 775–784. https://doi.org/10.1016/j.advwatres.2004.05.007

Malik, R. S., Anlauf, R., & Richter, J. (1992). A simple model for predicting evaporation from bare soils. *Zeitschrift für Pflanzenernährung und Bodenkunde*, *155*(4), 293–299. https://doi.org/10.1002/jpln.19921550409

Maltsev, T. (1954). *New system of soil cultivation and sowing*. Moscow: Znanie. (in Russian)

Mehari, A., Van Steenbergen, F., & Schultz, B. (2011). Modernization of spate irrigated agriculture: A new approach. *Irrigation and Drainage*, *60*(2), 163–173. https://doi.org/10.1002/ird.565

Minhas, P. S., Khosla, B. K., & Prihar, S. S. (1986). Evaporation and redistribution of salts in a silt loam soil as affected by tillage induced soil mulch. *Soil and Tillage Research*, *7*(4), 301–313. https://doi.org/10.1016/0167-1987(86)90018-8

Mualem, Y., & Assouline, S. (1989). Modeling soil seal as a nonuniform layer. *Water Resources Research*, *25*(10), 2101–2108. https://doi.org/10.1029/WR025i010p02101

Novák, V. (2012). *Evapotranspiration in the Soil-Plant-Atmosphere System*. Dordrecht: Springer. https://doi.org/10.1007/978-94-007-3840-9

Novakovska, I., Bulgakov, V., Rucins, A. & Dukulis, I., (2018). Analysis of soil tillage by ploughs and optimization of their aggregation. Engineering for Rural Development, 335–341 DOI: https://doi.org/10.22616/ERDev2018.17.N401

Ovsinsky, I. E. (1899). *A new system of agronomy*. Kiev. (in Russian)

Philip, J. R. (1969). Theory of infiltration. *Advances in Hydroscience*, *5*, 215–296. https://doi.org/10.1016/B978-1-4831-9936-8.50010-6

Philip, J. R. (1991). Upper bounds on evaporation losses from buried sources. *Soil Science Society of America Journal*, *55*(6), 1516–1520. https://doi.org/10.2136/sssaj1991.03615995005500060002x

Polubarinova-Kochina, P. Y. (1962). *Theory of ground water movement*, (2nd edition of the book ed.). Princeton: Princeton University Press. (in Russian) was published in 1977, Nauka, Moscow

Price, J., Rochefort, L., & Quinty, F. (1998). Energy and moisture considerations on cutover peatlands: Surface microtopography, mulch cover and Sphagnum regeneration. *Ecological Engineering*, *10*(4), 293–312. https://doi.org/10.1016/S0925-8574(98)00046-9

Prihar, S. S., Jalota, S. K., & Steiner, J. L. (1996). Residue management for reducing evaporation in relation to soil type and evaporativity. *Soil Use and Management*, *12*(3), 150–157. https://doi.org/10.1111/j.1475-2743.1996.tb00536.x

Pykhtin I.G., (2017). Tillage: Reality and myths. Zemledelie. No 1. 33–36 (in Russian) https://cyberleninka.ru/article/n/obrabotka-pochvy-deystvitelnost-i-mify

Ripple, C. D., Rubin, J., & Van Hylckama, T. E. A. (1970). *Estimating steady-state evaporation rates from bare soils under conditions of high water table*. Menlo Park, CA: USGS, Water Resources Division.

Sadeghi, M., Tuller, M., Gohardoust, M. R., & Jones, S. B. (2014). Column-scale unsaturated hydraulic conductivity estimates in coarse-textured homogeneous and layered soils derived under steady-state evaporation from a water table. *Journal of Hydrology*, *519*, 1238–1248. https://doi.org/10.1016/j.jhydrol.2014.09.004

Salvucci, G. D. (1993). An approximate solution for steady vertical flux of moisture through an unsaturated homogeneous soil. *Water Resources Research*, *29*(11), 3749–3753. https://doi.org/10.1029/93WR02068

Schwartz, R. C., Baumhardt, R. L., & Evett, S. R. (2010). Tillage effects on soil water redistribution and bare soil evaporation throughout a season. *Soil and Tillage Research*, *110*(2), 221–229. https://doi.org/10.1016/j.still.2010.07.015

Shi, W. J., Shen, B., & Wang, Q. J. (2014). Effect of ignoring parameter b on the maximum upward flux calculated from the Gardner rational model. *Canadian Journal of Soil Science*, *94*(1), 97–103. https://doi.org/10.4141/cjss2013-029

Šimůnek, J., van Genuchten, M. T., & Šejna, M. (2016). Recent developments and applications of the HYDRUS computer software packages. *Vadose Zone Journal*, *15*(7), 25. https://doi.org/10.2136/vzj2016.04.0033

Soylu, M. E., Istanbulluoglu, E., Lenters, J. D., & Wang, T. (2011). Quantifying the impact of groundwater depth on evapotranspiration in a semi-arid grassland region. *Hydrology and Earth System Sciences*, *15*(3), 787–806. https://doi.org/10.5194/hess-15-787-2011

Stewart, J. M., & Broadbridge, P. (1999). Calculation of humidity during evaporation from soil. *Advances in Water Resources*, *22*(5), 495–505. https://doi.org/10.1016/S0309-1708(98)00024-4

Strudley, M. W., Green, T. R., & Ascough, J. C. (2008). Tillage effects on soil hydraulic properties in space and time: State of the science. *Soil and Tillage Research*, *99*(1), 4–48. https://doi.org/10.1016/j.still.2008.01.007

Turusov, V.I., Garmashov, V.M., Kornilov, I.M. & Nuzhnaya, N.A., (2018). Agro-bioenergy efficiency of various pea soil basic management practices under conditions of the south-east of the Central Chernozem Zone. Proceedings Michurin's State Agrarian University, 6-10. http://www.mgau.ru/sciense/journal/PDF_files/vestnik_2_2018.pdf#page=10

Unger, P. W., & Cassel, D. (1991). Tillage implement disturbance effects on soil properties related to soil and water conservation: A literature review. *Soil and Tillage Research*, *19*(4), 363–382. https://doi.org/10.1016/0167-1987(91)90113-C

van Genuchten, M. Th. (1980). A closed form equation for predicting the hydraulic conductivity of unsaturated soils. *Soil Science Society of America Journal*, *44*, 892–898.

Verburg, K., Bond, W. J., & Hunt, J. R. (2012). Fallow management in dryland agriculture: Explaining soil water accumulation using a pulse paradigm. *Field Crops Research*, *130*, 68–79. https://doi.org/10.1016/j.fcr.2012.02.016

Verhulst, N., Govaerts, B., Verachtert, E., Castellanos-Navarrete, A., Mezzalama, M., Wall, P., et al. (2010). Conservation agriculture, improving soil quality for sustainable production systems. In *Advances in soil science: Food security and soil quality*, (pp. 137–208). Boca Raton: CRC press.

Warrick, A. W. (1988). Additional solutions for steady-state evaporation from a shallow water table. *Soil Science*, *146*(2), 63–66. https://doi.org/10.1097/00010694-198808000-00001

Warrick, A. W. (2003). *Soil water dynamics*. New York: Oxford University Press.

Warrick, A. W., & Yeh, T. C. J. (1990). One-dimensional, steady vertical flow in a layered soil profile. *Advances in Water Resources*, *13*(4), 207–210. https://doi.org/10.1016/0309-1708(90)90042-3

Wendroth, O., & Wypler, N. (2008). Unsaturated hydraulic properties: Laboratory evaporation. In M. R. Carter & E. G. Gregorich (Eds.), *Soil sampling and methods of analysis* (Chap. 81, pp. 1089–1127). Boca Raton, FL: CRC Press.

Willis, W. O. (1960). Evaporation from layered soils in the presence of a water table. *Soil Science Society of America Journal*, *24*(4), 239–242. https://doi.org/10.2136/sssaj1960.03615995002400040009x

Willis, W. O., & Bond, J. J. (1971). Soil water evaporation: Reduction by simulated tillage. *Soil Science Society of America Journal*, *35*(4), 526–529. https://doi.org/10.2136/sssaj1971.03615995003500040016x

Wolfram, S. (1991). *Mathematica. A system for doing mathematics by computer*. Redwood City: Addison-Wesley.

Wuest, S. B., & Schillinger, W. F. (2011). Evaporation from high residue no-till versus tilled fallow in a dry summer climate. *Soil Science Society of America Journal*, *75*(4), 1513–1519. https://doi.org/10.2136/sssaj2010.0368

Xiao, B., Zhao, Y. G., & Shao, M. A. (2010). Characteristics and numeric simulation of soil evaporation in biological soil crusts. *Journal of Arid Environments*, *74*(1), 121–130. https://doi.org/10.1016/j.jaridenv.2009.06.013

Yadav, G. S., Saha, P., Babu, S., Das, A., Layek, J., & Debnath, C. (2018). Effect of no-till and raised-bed planting on soil moisture conservation and productivity of summer maize (zea mays) in Eastern Himalayas. *Agricultural Research*, *7*(3), 300–310. https://doi.org/10.1007/s40003-018-0308-8

Yuan, C., Lei, T., Mao, L., Liu, H., & Wu, Y. (2009). Soil surface evaporation processes under mulches of different sized gravel. *Catena*, *78*(2), 117–121. https://doi.org/10.1016/j.catena.2009.03.002

Zarei, G., Homaee, M., Liaghat, A. M., & Hoorfar, A. H. (2010). A model for soil surface evaporation based on Campbell's retention curve. *Journal of Hydrology*, *380*(3-4), 356–361. https://doi.org/10.1016/j.jhydrol.2009.11.010

Zhou, Y., & Rowe, R. K. (2005). Modeling of clay liner desiccation. *International Journal of Geomechanics*, *5*(1), 1–9. https://doi.org/10.1061/(ASCE)1532-3641(2005)5:1(1)